Investigation of a Reattaching Turbulent Shear Layer: Flow Over a Backward-Facing Step

J. Kim[1]
S. J. Kline
J. P. Johnston

Department of Mechanical Engineering
Stanford University
Stanford, Calif.

Incompressible flow over a backward-facing step is studied in order to investigate the flow characteristics in the separated shear-layer, the reattachment zone, and the redeveloping boundary layer after reattachment. Two different step-heights are used: $h/\delta_s = 2.2$ and $h/\delta_s = 3.3$. The boundary layer at separation is turbulent for both cases. Turbulent intensities and shear stress reach maxima in the reattachment zone, followed by rapid decay near the surface after reattachment. Downstream of reattachnent, the flow returns very slowly to the structure of an ordinary turbulent boundary layer. In the reattached layer the conventional normalization of outer-layer eddy viscosity by $U_\infty \delta^*$ does not collapse the data. However, it was found that normalization by $U_\infty(\delta - \delta^*)$ does collapse the data to within ± 10% of a single curve as far downstream as $x/x_R \approx 2$, the last data station. This result illustrates the strong downstream persistence of the energetic turbulence structure created in the separated shear layer.

Introduction

Separation of turbulent flows has received a great deal of attention because of its practical importance; nevertheless, it is still far from well understood. Relatively little effort, moreover, has been allocated to flow downstream of separation, and even less to that downstream of reattachment. In many real flows, separation of a boundary layer is followed downstream by reattachment of the separated layer to a solid surface. Understanding the characteristics of reattachment and the redeveloping boundary layer, therefore, becomes a significant problem in engineering applications (e.g., diffuser flows, flows over aircraft wings). In addition, separation and reattachment of a turbulent shear-layer provides a basic flow situation against which many existing theories and models of turbulence can be tested and possibly improved.

The separation-reattachment process is characterized by a complex interaction between the separated shear-layer and the adjacent flow. The most important changes in interaction condition depend on whether the flow is laminar or turbulent at separation and at reattachment. Three different flow regimes are possible: (1) laminar-laminar, where the boundary layer flow is laminar at both separation and reattachment; (2) laminar-turbulent, where flow is laminar at separation and turbulent at reattachment; and (3) turbulent-turbulent, where flow is turbulent at both separation and reattachment. The present experiment belongs to category (3).

Flow over a backward-facing step was used in this study because of its simple geometry. The separation point is fixed by a sharp corner with this geometry. Hence the process of separation-reattachment can be examined without any complexities resulting from motion of the separation point.

Because of the practical importance of predicting base pressure of bluff bodies moving with high speed (such as bullets and coasting missiles), aeronautics researchers have long been interested in the flow over a backward-facing step. Due to the nature of the field, however, much of the work has been done in supersonic flow, where the central problem becomes the shockwave boundary layer interactions. A relatively limited number of studies in low-speed flow over a backward-facing step exists in the literature (see references [1 to 11]. A brief review of the main characteristics of most of the flows and those of some other related flows investigated in the above studies can be found in reference [12].

The purpose of the present study are

- to investigate flow characteristics in the separated shear layer, the reattachment zone, and the redeveloping boundary layer downstream of reattachment;
- to increase understanding of the separation-reattachment process; and
- to obtain new experimental data that may be used to develop computational models.

Experimental Facility

The wind tunnel used in this experiment was the same as that used by Chui and Kline [13], except for the filter box and test section. The filter box described in Hussain and Reynolds [14] was used to insure a supply of clean air needed for hot-wire measurements.

The end of the tunnel was shaped to form a contraction nozzle of ratio 18 to 1. The end of the nozzle was 7.62 cm (3 inches) wide and 60.96 cm (24 in.) high. A new test section

[1] Present address: NASA-Ames Research Center, Moffett Field, Calif.

Contributed by the Fluids Engineering Division of THE AMERICAN SOCIETY OF MECHANICAL ENGINEERS and presented at the Winter Annual Meeting, New York, N.Y., December 2-7, 1979. Manuscript received by the Fluids Engineering Division, April 2, 1979.

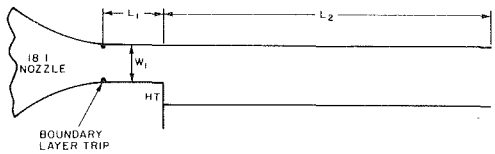

W_1 = INLET WIDTH 3 in. (7.62 cm)
L_1 = INLET LENGTH 12 in. (30.48 cm)
L_2 = TEST SECTION 92 in. (233.68)
HT = ADJUSTABLE STEP HEIGHT 0–8 in. (0–20.32 cm)

Fig. 1 Schematic of test section

was built and attached to the tunnel. The dimensions of the test section are shown in Fig. 1. At the beginning of the inlet, boundary layer trips were placed on each side wall. The trips were carefully machined from phenolic strips to assure that the tripped bounary layer remained two-dimensional.

Pressure was measured by a manometer and a transducer. A Combist micromanometer, using 0.82 s.g. oil with an uncertainty of ± 0.013 mm of water, was used as the standard for pressure measurement. A Validyne DP45 variable reluctance differential pressure transducer, with a diaphragm rating for a maximum pressure of 25.4 mm of water (250 NT/m^2), was calibrated against the micromanometer and used for most of the pressure measurements. The calibration curve of the transducer was checked several times during a run; it was found to be stable and linear within ± 0.025 mm of water.

Since there was a pressure gradient across the shear layer, static pressure variation normal to the wall was also measured. A tubular static pressure probe was made out of 3.18 mm stainless steel tubing. The probe was calibrated against a wall pressure tap in the region where there was no pressure gradient normal to the wall. Total pressure was measured by a C-shaped impact probe made of a 25-gauge (0.51 mm O.D.) hypodermic tubing. This probe was calibrated against a United Sensor and Control Corporation type KA kiel probe.

Thermo-Systems, Inc. (TSI) Model 1050 constant-temperature anemometers together with TSI Model 1052 polynomial linearizers were used as the basic anemometer systems. A TSI Model 1076 RMS meter was used for measurement of turbulence intensities, and multiplications were performed by a DISA Model 52B25 Turbulence Processor to obtain Reynolds shear stress, $\overline{u'v'}$. A TSI Model 1243 boundary layer x-probe of 4-micron, platinum-coated tungsten wire was used for turbulence measurement. This probe was calibrated at the centerline of the channel at the reference point (x = -15.24 cm^2), where the velocity is uniform across the central region of the channel; the calibration was performed each time before the measurement to minimize the effect from the variation of the ambient temperature of the tunnel.

A special unit was designed and built to measure the intermittency directly. A description of the unit can be found in Kim, et al. [12]. As a qualification test, intermittency of a flat-plate turbulent boundary layer was measured and compared with that obtained by Fiedler and Head [15]. The two results were in good agreement.

Experimental Conditions

The experiment was performed with two different step-heights, 3.81 cm (1.5 in.) and 2.54 cm (1 in.), which are labeled REF and STEP-1, respectively. These step-heights gave aspect ratios (step span to height, b/h) of 16 and 24, respectively, which are higher than the value 10 recommended by de Brederode and Bradshaw [7] as the minimum to assure two-dimensionality of flow in the central region, away from the end-wall bondary layers. The reference dynamic pressure, measured in the inviscid core at the reference point, was kept the same for both experiments at a value of 20.3 mm of water. The reference speed, therefore, varied slightly, depending upon atmospheric conditions in the laboratory. The typical reference speed was 18.2 m/s, with a variation less than 0.15 m/s throughout the experiment. The velocity profile at the reference point (x = -15.24 cm) was that of an equilibrium turbulent flat-plate profile, and the boundary layer displacement thickness at that point was 1.04 mm for both experiments. Reynolds number based on the momentum thickness at separation (x = 0) was about 1.3×10^3.

Experimental Results

Tufts and a mixture of oils were used to visualize the flow field and to determine the reattachment zone. Only a small part of the separated flow (about one step-height length in the middle of the recirculating zone) at $x/h \approx 3$ was found to be steady. Most of the recirculating zone contained unsteady flow, even though it is often called the "dead air zone." Near reattachment, flow was highly unsteady and the tufts moved forward and backward continuously, indicating the variation of the instantaneous reattachment length. The mean distance to reattachement was found to be $x_R/h = 7 \pm 1$. A series of still photographs of the tufts revealed the instantaneous reattachment length was not a straight line across the span; however, it was a straight line in the mean, as indicated by wall oil-flow visualization. This might be indicative of the existence of a three-dmensional spanwise structure near reattachment, but this suggestion was not investigated in detail (see reference [16] for further study).

The wall-static pressure on the step side of the channel for

[2] The step location, x = 0.

Nomenclature

b = channel height (span)
C_p = static pressure coefficient
h, HT = step height
l = turbulent mixing length
p = static pressure
Re_θ = Reynolds number based on θ, $U_\infty \theta/\nu$
U, u = mean velocity in x-direction
u' = turbulent fluctuation in x-direction
u_τ = wall shear velocity $(\tau_w/\rho)^{1/2}$
u^+ = u/u_τ
v' = turbulent fluctuation in y-direction
W_1 = inlet channel width
x = coordinate in streamwise direction
y = coordinate normal to the wall
y^+ = yu_τ/ν
γ = intermittency of turbulence
δ = boundary layer thickness
δ^* = displacement thickness
θ = momentum thickness
ν = kinematic viscosity
ν_T = eddy viscosity
τ = turbulent shear stress $(= -\rho\overline{u'v'})$

Subscripts

s = value at separation
R = value of reattachment
o = reference condition (x = − 15.24 cm)
∞ = free-stream value

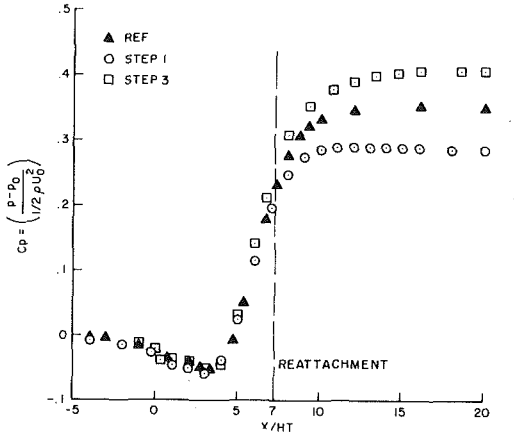

Fig. 2 Step-side pressure distributions for different step-heights

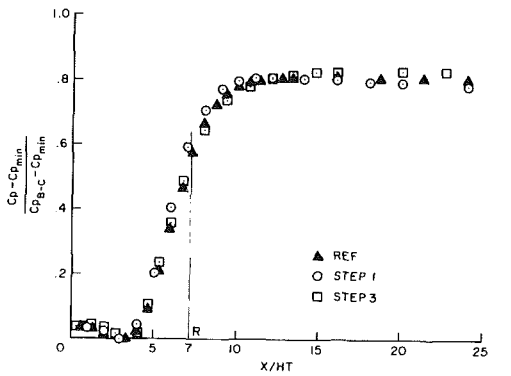

Fig. 3 Normalized pressure coefficients

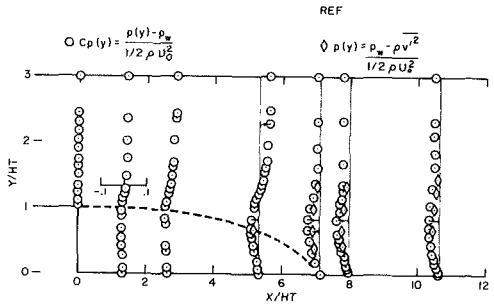

Fig. 4 Static pressure variation across the channel

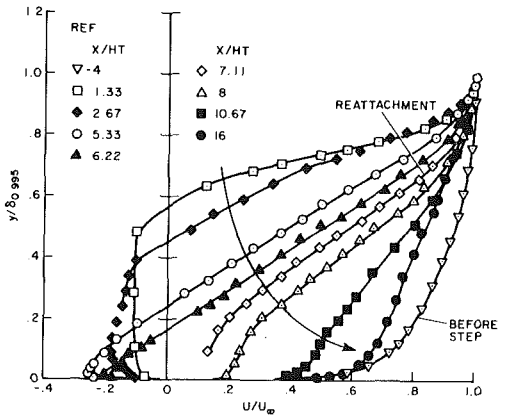

Fig. 5 Velocity profiles on the step-side: U/U_∞ versus y/δ

three different step-heights is shown in Fig. 2.[3] In this figure, the static pressure is plotted in the form of the pressure coefficient,

$$C_p = \frac{p - p_0}{\frac{1}{2}\rho U_0^2} \tag{1}$$

where p_0 and U_0 are the reference pressure and the free stream velocity, respectively, measured at x = - 15.24 cm. The streamwise distance x measured along the surface has its origin, $x = 0$, at the step and is non-dimensionalized by the step heights. Pressure increases for a short distance beyond the reattachment; the final pressure recovery is a function of downstream channel width. In an attempt to normalize the variations due to the different channel widths. A new normalized pressure coefficient was defined as

$$C_p = \frac{C_p - C_{p_{\min}}}{C_{p_{B-C}} - C_{p_{\min}}} \tag{2}$$

where $C_{p_{B-C}}$ is the Broda-Carnot pressure coefficient.[4] The normalizaton (2) reduces the data to a single curve, as shown in Fig. 3.

The static pressure variation across the channel is shown for the REF case in Fig. 4. The static pressure data were not corrected for turbulence effect because the effect of turbulence on the static pressure reading is not well understood. In order to show the variation of the static pressure normal to the surface, the pressure coefficient was defined as

$$C_p(t) = \frac{p(y) - p_w}{\frac{1}{2}\rho U^2{}_0} \tag{3}$$

where p_w is the static pressure on the surface at a given streamwise location.

The mean velocity profiles on the step-side of the channel are shown in Fig. 5. The parts of the velocity profiles in the recirculating region were obtained by placing the total pressure probe with its mouth facing the direction of local mean flow. This procedure will of course not give true reversed velocity if the flow changes its direction during the measurement, and in fact the flow changes its direction continuously near reattachment. No attempt to correct for this effect was made in the present experiment,[5] and the experimental uncertainty[6] (20:1 odds) in the measurements of the region of reversed flow was estimated to be about 10% of the measured values. In Fig. 6, the mean velocity profiles downstream of reattachment are plotted in terms of the non-dimensionalized variables, u^+ versus y^+. Wall shear stress, u_τ, was determined by the "cross-plot" method.[7] (Wall shear stresses measured by a Preston tube did not differ more than 5 percent from the value obtained by this method.)

Turbulence profiles along the channel are shown in Fig. 7.

[3] Data for STEP-3, the 7.62 cm step-height, were provided by J. Eaton, using the same apparatus and technique.

[4] $C_{p_{B-C}} \triangleq 2\frac{1}{AR}\left(1 - \frac{1}{AR}\right)$,

Where AR is the area ratio between upstream and downsteam of the channel.

[5] Such measurements are being pursued in a later study by J. Eaton, to be reported separately.

[6] The experimental uncertainties were estimated following the procedure of Kline and McClintock [17].

[7] The wall shear stress is found by forcing data points to match the logarithmic profile ($u^+ = (1/0.41 \cdot \ln y^+ + 5.0)$ over the range of y^+ of 50 to 170. See Schraub and Kline [18] for details.

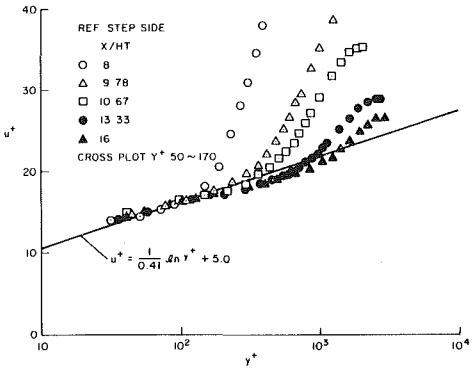

Fig. 6 Mean velocity profiles (step-side): y^+ versus u^+

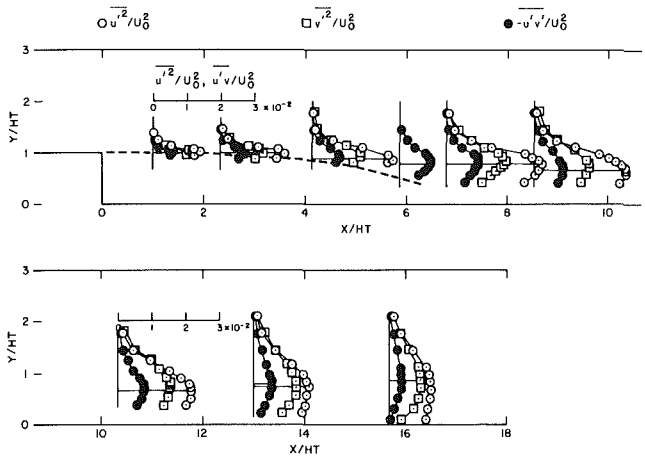

Fig. 7 Turbulent profiles along the channel (REF) (Tabulated data are available in reference [12])

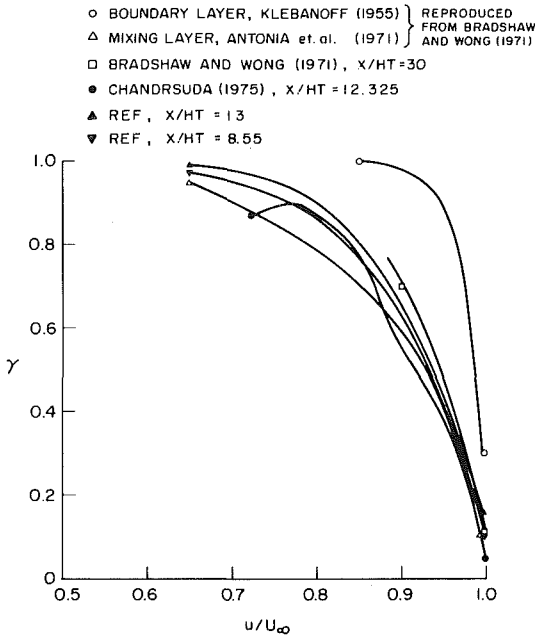

Fig. 8 Comparison of profiles of intermittency

The turbulence measurements were not made in the regions where significant errors were expected, due to signal rectification as a result of the directional insensitity of the hot-wire. At the lowest point of transverse in the figure, $\sqrt{\overline{u'^2}}/U$ was about 40 percent and $\sqrt{\overline{u'^2}_{\max}}/U$ was about 30 to 40 percent. The estimated experimental uncertainties of $\overline{u'^2}$, $\overline{v'^2}$, and $\overline{u'v'}$ were less than 10 percent of the measured values in the region where $\sqrt{\overline{u'^2}}/U$ was less than 0.2, while the uncertainties were about 20 percent when $\sqrt{\overline{u'^2}}/U$ was about 0.4

Intermittency, γ, was measured using $d/dt(u'v')$ as a criterion function. After Bradshaw and Murlis [19], the "signal-or-derivative" approach is used to separate turbulent and nonturbulent flow—that is, flow is declared to be turbulent if either the signal or its derivative exceeds a preset threshold (see Kim, et al. [12] for details). Intermittency profiles of a mixing layer, the redeveloping boundary layer downstream of reattachment, and an ordinary turbulent boundary layer are shown in Fig. 8.

Discussion of Experimental Results

The general flow characteristics hardly changed for the two different step-heights. The effect of change in Reynolds number over a limited range was negligible; this is consistent with previous results obtained by Tani, et al. [1], Abbott and Kline [3], and Chandrsuda [9]. This finding is in constrast to the case of laminar separation with laminar reattachment or laminar separation, where transition does not occur near the step edge. In these cases, flow depends on the step-height and Reynolds number, as observed by Moore [2] and Goldstein et al. [5].

At least for narrow channels where $W_1/h \approx 1$,[8] the values of mean reattachment length $x_R/h = 7 \pm 1$ seem to be universal when flow is turbulent at separation or when the transition to turbulence occurs very close to separation. The flow near reattachment is unsteady, however, and the instantaneous reattachment point is not fixed but moves around within a range. Hence, it seems more appropriate to refer to it as a reattachment "zone" rather than a reattachment point. Since the reattachment length is related directly to the entrainment rate, this suggests that entrainment in the mixing layer does not take place at a uniform rate, but fluctuates. Note that a higher entrainnment rate results in a smaller reattachment length, and vice versa. This is consistent with the observation that distance to reattachment may be quite long for laminar-laminar cases.

As mentioned previously, normalization using a parameter $\hat{C}_p$ reduces the wall pressure data to a single curve. Hence the correlation can be used for an estimation of the pressure recovery of similar geometries, since $C_{p_{B-C}}$ is known for a given geometry and $C_{p_{\min}}$ varies only slightly.

Static pressure increases beyond reattachment, as shown in Fig. 3. This effect can be explained by evaluating the x-momentum equation on the surface; this yields a balance between pressure force and shear force. That is,

$$\frac{1}{\rho}\frac{\partial p}{\partial x} = \frac{\partial \tau}{\partial y} \tag{4}$$

where τ is the total shear stress. In the zone of reattachment this requires positive $\partial p/\partial x$, because the shear stress rises from a typical boundary layer value to a typical mixing layer value near the surface.

The variation of the static pressure across the channel (see Fig. 4) has two causes: the streamline curvature and the high turbulence intensity. The effect of turbulence on the pressure

[8] Examination of other cases (see reference [12] for $\mathrm{Re}_{\theta_s} \gtrsim 1000$ and strong to overwhelming perturbation ($\delta_s < h$) shows that distance to reattachment also depends upon channel width to step-height, W_1/h. For channels like ours ($W_1/h \approx 1$), $x_R \approx 7$, but for very wide channels ($W_1/h \approx 10$), shorter reattachment lengths are typical, e.g., $x_R/h \approx 5.5$ to 6.0. This effect is believed to result from viscid-inviscid flow outside the reattaching shear geometry changes which affect the inviscid flow outside the reattaching shear layer more than they affect the turbulence structure itself.

can be obtained form the y-momentum equation. With the usual boundary layer approximation to the Navier-Stokes equation, but including the turbulence term, the y-momentum equation reduces to

$$\frac{\partial p}{\partial y} = -\frac{\partial}{\partial y}\rho\overline{v'^2} \tag{5}$$

or

$$p(y) = p_w - \rho\overline{v'^2} \tag{6}$$

The y-variation of the static pressure coefficent due to the turbulent fluctuations then becomes

$$C_p(y) = \frac{p(y) - p_w}{\frac{1}{2}U_0^2} = -2\frac{\overline{v'^2}}{U_0^2} \tag{7}$$

This effect is shown by the diamond-shaped points in Fig. 4. Near reattachment a large portion of the cross-term variation of static pressure appears to be caused by the turbulent fluctuations. At $x/h = 7.1$, for example, the maximum variation of $C_p(y)$ is about 6 percent of $(1/2)\rho U_0^2$; of this, 4 percent appears to be caused by the turbulent normal stress, $\rho\overline{v'^2}$. Far downstream of reattachnent, most of the variation is accounted for by the turbulence effect.

The mean velocity profiles shown in Fig. 5 exhibit the typical features of flow over a backward-facing step. The velocity profile before the step is that of an ordinary turbulent boundary layer with shape factor $H = \delta^*/\theta = 1.4$. The magnitude of reversed velocities in the recirculating flow is on the order of 10 to 20 percent of U_0; this result agrees with Tani, et al. [1] and Chandrsuda [9]. The maximum reversed velocity measured is about 25% of free-stream velocity. Downstream of reattachment, the velocity profile returns toward the ordinary turbulent boundary layer. The inner part of the profile relaxes rather quickly, while the outer part requires a surprisingly long distance. The rapid increase of the velocity near the surface downstream of reattachment and the slow response of the layer away from the surface produce an appreciable decrease in mean-velocity gradient in the region above $y^+ \approx 100$. This results in a marked dip in the data below the universal inner-layer profile, this logarithmic law, as shown in Fig. 6, indicating that the flow here is not in local equilibrium. It appears that the local wall-shear velocity, u_τ, which is used as an inner-layer scaling in the local equilibrium flow, is no longer the proper inner velocity scale throughout the layer, since only the velocity very close to the surface adjusts rapidly to the sudden change of the boundary condition, i.e., the reattachment. The velocity away from the surface, on the other hand, responds slowly to the change, causing the dip below the log-law.

The lower velocity gradient is rather puzzling, as pointed out by Bradshaw and Wong [6], since the local equilibrium formula,

$$\frac{\partial U}{\partial y} = \frac{(\tau/\rho)^{1/2}}{\kappa y} \tag{8}$$

would give a velocity gradient even higher than the logarighmic value $(\tau_w/\rho)^{1/2}/\kappa y$ obtained from the log-law in the region $y/\delta < 0.2$, and the formula should hold, since τ is increasing away from the surface. They suspected that the turbulent length scale in the region may not be κy, but rather that it will increase much more rapidly with y. The turbulent mixing length was obtained from the results of the present experiment and is shown in Fig. 9. The mixing length is found to be much larger than κy at $y/\delta < 0.2$. This is understandable, because part of the separated shear layer, which

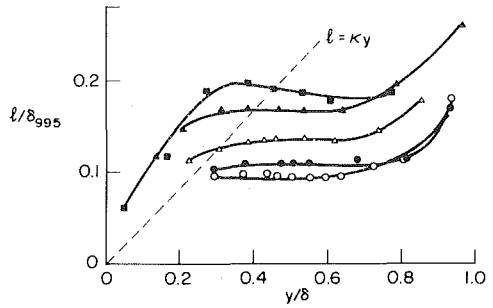

Fig. 9 Turbulent mixing length downstream of reattachment -- REF

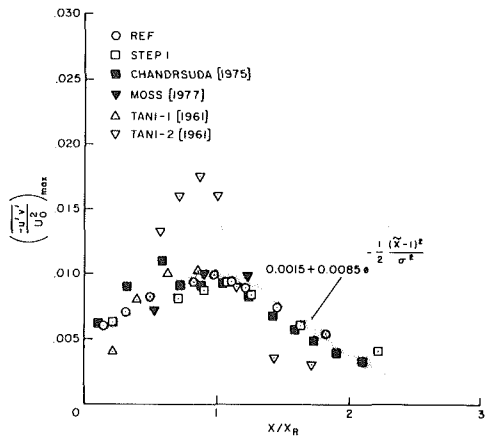

Fig. 10 Distribution of maximum shear stress

has a larger mixing length than the usual attached layer value near the surface, comes very close to the surface as the flow proceeds through reattachment. Therefore, the turbulent length scale can be very large, very close to the surface, even though it decreases to zero at the surface. The result is a mean-velocity gradient lower than that predicted by equation (8), and hence the dip in u^+ below the log-law, as shown in Fig. 6.

The lines which denote the locations of maximum turbulent energy and shear stress coincide with the dividing streamline initially; they deviate outward as the reattachment is approached. Downstream of reattachment near the surface, strong, local, longitudinal rates of strain, $\partial U/\partial x$, increase $\overline{v'^2}$ and $\overline{w'^2}$ and decrease $\overline{u'^2}$. Because of this effect, the difference in the magnitude between $\overline{u'^2}$ and $\overline{v'^2}$ decreases downstream of reattachment. The area between profiles of $\overline{u'^2}$ and $\overline{v'^2}$ in Fig. 7 represents

$$\int_0^\delta (\overline{u'^2} - \overline{v'^2})\, dy,$$

whose streamwise gradient appears in the momentum integral equation. It is apparent that

$$\frac{\partial}{\partial x}\int_0^\delta (\overline{u'^2} - \overline{v'^2})\, dy$$

is not negligible near reattachment. The measurements of the present experiment do not allow accurate quantitative evaluation of this term; however, it should be included in the momentum integral equation if this equation is used for analysis.

The maximum values of turbulent intensities and shear stress have a consistent trend, i.e., a monotonic increase toward a peak value at a station very close to reattachment, followed by a rapid decay downstream of reattachment suggesting a significant change in the structure of the shear layer. At $x/h = 15.67$, the shear stress drops to less than half its value at reattachment. The streamwise variation of the

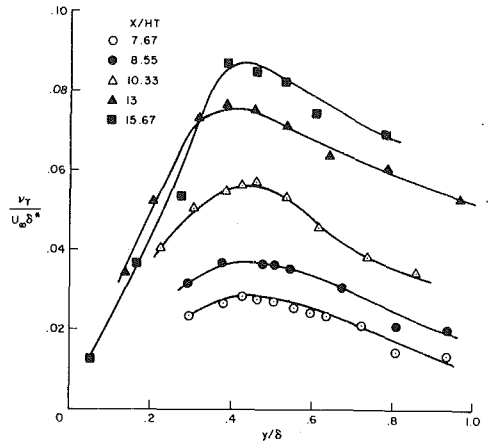

Fig. 11 Nondimensionalized eddy viscosity (REF) using typical correlation

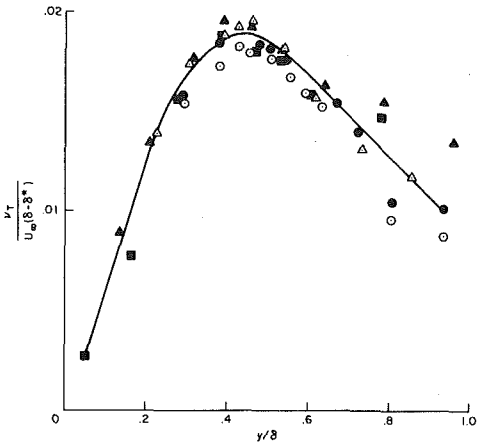

Fig. 12 Nondimensionalized eddy viscosity (REF) using new correlation

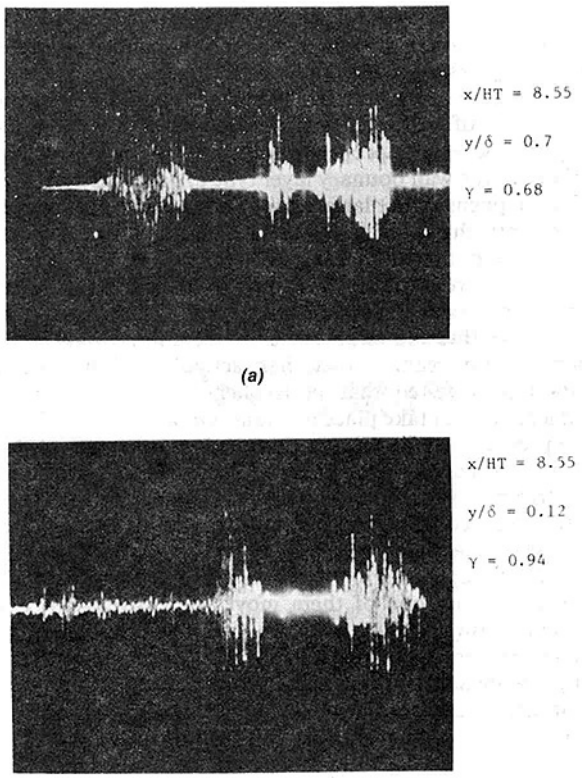

Fig. 13 Photographs of $d/dtu'v'$ from oscilloscope fall

maximum shear stress from different experiments is shown in Fig. 10. $\bar{x}$, defined as x/x_R, is used as the abscissa in order to normalize the variation in the reattachment length. Except for the case of Tani-2, it is seen that the data can be approximated fairly well by a Gaussian curve, drawn such that it has a maximum value of $(-\overline{u'v'}/U_0^2)_{max} = 0.1$ at reattachment and approaches a value of $(-\overline{u'v'}/U_0^2)_{max} = 0.0015$ far downstream of reattachment. This correlation has been used successfully in the computation of the flow over a backward-facing step [12].

The eddy viscosity, defined as $\nu_T = -\overline{u'v'}/(dU/dy)$, is shown in Fig. 11 for the attached flow downstream of reattachment. The eddy viscosity is non-dimensionalized in terms of $U_\infty\delta^*$, the method typically used for attached boundary layers close to equilibrium. This procedure usually colllapses the eddy viscosities in the outer 80 percent of the layer into a nearly universal curve which varies only slightly with pressure gradients. It is apparent in Fig. 11 that this type of collapse does not occur downstream of reattachment. A new non-dimensionalization was therefore formed in terms of $U_\infty(\delta-\delta^*)$, as shown in Fig. 12. (Note that the regression line is drawn through the data as a visual aid.) The result of this new nondimensionalization looks quite satisfactory. It is universal to within the experimental uncertainty. The failure of the conventional correlation is due to the unusual nature of the redeveloping boundary layer downstream of reattachment. In most flow, δ^* increases as U_∞ decreases, so that $U_\infty\delta^*$ tends to remain unchanged. Downstream of reattachment, however, both U_∞ and δ^* decrease and consequently $\nu_T/U_\infty\delta^*$ increases. The new scaling length $(\delta-\delta^*)$, increases downstream of reattachment; it seems to be an appropriate choice for a new characteristic length. Computational results using this correlation have been very satisfactory in predicitng flows downstream of reattachment (see reference [12]).

The characteristics of the outer-layer structure, which is dominated by large turbulent eddies, can be compared to those of other turbulent shear flows by examining the intermittency profiles. Intermittency profiles of different shear flows are shown in Fig. 8. The profiles of the reattaching flow lie between those of the free mixing layer and the ordinary turbulent boundary layer, and they develop very slowly toward the profile of an ordinary boundary layer. The outer layer of reattaching flow is dominated by large and energetic eddies typical of free shear layer flow. These eddies have a relatively long lifetime and carry the "history effect" of the upstream flow. Hence the outer layer takes a relatively long time to return to the ordinary structure of a turbulent boundary layer. Fig. 8 manifests the slow return to the ordinary structure.

The criterion function used for the intermittency measurements, i.e., $d/dt(u'v')$. was monitored through an oscilloscope during the measurement. Typical results are shown in Fig. 13. The characteristic of intermittent turbulent flow is seen in the first figure, which was taken at the outer edge of the shear layer at $x/h = 8.55$ and $y/\delta = 0.7$. The intermittency at this point was about 0.6. The lower picture was taken at $x/h = 8.55$ and $y/\delta = 0.12$. Note that $x/h = 8.55$ is downstream of but close to reattachment. Two different structures are seen in the signal at $y/\delta = 0.12$; they seem to represent two different turbulent flows (measured intermitendency was close to 1.0). The bigger spikes have the same structure as the approaching shear layer; however, the small spikes seems to be the structure of the normal boundary layer. This structure (that is, a signal which is intermittent between two different forms of turbulence) contrasts sharply

with the intermittency of an ordinary boundary layer, which is intermittent between turbulent and non-turbulent zones of fluid. It appears that this might be the reason for the rapid decay of $-\overline{u'v'}$ and other time-averaged turbulent intensities downstream of reattachment, since, through the time-averaged process, the properties of the free shear layer type and those of the wall bounary layer type are averaged out.

What happens to the large eddies in the approaching shear layer at reattachment is not yet clear. Bradshaw and Wong [6] suggested that the large eddies are torn into two parts at reattachment, resulting in a significant decrease in the turbulent length scale downstream of reattachment. Another possibility is that the large eddies move alternatively downstream and upstream, rather than actually splitting. Chandrsuda [9] suggested that both phenonmena seems to be possible, and both take place in a random fashion. The results of the present experiment, e.g., unsteady movements of tufts near the reattachment zone and the structure of $d/dt(u'v')$ downstream of reattachment, seem to support the hypothesis of alternating eddies; the probe downstream of reattachment should see the large spikes in Fig. 13 *continuously,* if the large eddies in the approaching shear layer were torn in two at reattachment and one of them moves downstream of reattachment. However, the evidence presented here does not exclude the hypothesis of splitting, nor of the existence of both phenomena. All that can be said at this point about the fate of large eddies is that it is unlikley that the splitting is the only phenomenon that takes place at reattachment.

Summary

Measurements were made in a low-speed flow over a backward-facing step. Although the instruments used in his study prevented extensive measurements in the recirculating flow (and also included a rather high experimental uncertainty), the present experimental study shows several features of the complex separation/reattachment process and the redeveloping boundary layer. Turbulent intensities and shear stress reach maxima in the reattachment zone, followed by rapid decay near the surface after reattachment. The very high time-averaged values of $\overline{u'v'}$ followed by the rapid decay downstream seem to be caused by the intermittent structure of the turbulence downstream of reattachment. Downstream of reattachment, the flow returns very slowly to the structure of an ordinary turbulent boundary layer. In the inner layer, the rapid adjustment of the velocity profile close to the surface causes a low mean-velocity gradient and, consequently, the dip below, the universal log-law. Eddy viscosity normalized by $\nu_T/U_\infty(\delta-\delta^*)$ is reduced to a single curve downstream of reattachment; however, the usual normalization using $\nu_T/U_\infty\delta^*$ does not collapse the data.

References

1 Tani, I., M. Iuchi, and H. Komodo, "Experimental Investigation of Flow Separation Associated with a Step or Groove," Report No. 364, 1961, Aeronautical Research Institute, University of Tokyo.

2 Moore, T. W. F., "Some Experiments on the Reattachment of a Laminar Boundary Layer Separating from a Rearward-Facing Step on a Flat Plate Aerofoil," *Journal of Royal Aeronautical Society,* Vol. 64, 1960, pp. 668-672.

3 Abbott, D. E., and S. J. Kline, "Theoretical and Experimental Ivestigation of Flow over Single and Double Backward-Facing Steps," MD-5, June 1961, Thermosciences Division, Dept. of Mechanical Engineering, Stanford University.

4 Mueller, T. J., and J. M. Robertson, "A Study of Mean Motion and Turbulence Downstream of a Roughness Element," *Proceedings of the First Southeastern Conference on Theoretical and Applied Mechaincs,* Galinberg, Tenn., 1962.

5 Goldstein, R. J., V. L. Eriksen, R. M. Olson, and E. R. G. Eckert," Laminar Separation, Reattachment, and Transition of Flow over a Downstream-Facing Step," *Journal of Basic Engineering,* Vol. 92, No. 4, 1970, pp. 732-741.

6 Bradshaw, P., and F. Y. F. Wong, "The Reattachment and Relaxation of a Turbulent Shear Layer," *Journal of Fluid Mechanics,* Vol. 52, Part 1, 1972, pp. 113-135.

7 de Brederode, U., and P. Bradshaw, "Three-Dimensional Flow in Nominally Two-Dimensional Separation Bubbles. I. Flow Behind a Rearward-Facing Step," IC Aero Report 72-19, 1972, Imperial College of Science and Technology.

8 Rothe, P. H., and J. P. Johnston, "The Effects of System Rotation on Separation, Reattachment, and Performance in Two-Dimensional Diffusers," PD-17, 1975, Thermosciences Division, Dept. of Mechanical Engineering, Stanford University.

9 Chandrsuda, C., "A Reattaching Turbulent Shear Layer in Incompressible Flow," Ph.D. thesis, 1975, Dept. of Aeronautics, Imperial College of Science and Technology.

10 Moss, W. D., S. Baker, and L. J. S. Bradbury, "Measurements of Mean Velocity and Reynolds Stresses in Regions of Recirculating Flow," presented at Symposium on Turbulent Shear Flows, Pennsylvania State University, 1977.

11 Etheridge, D. W., and P. H. Kemp, "Measurements of Turbulent Flow Downstream of a Rearward-Facing Step," *Journal of Fluid Mechanics,* Vol. 86, Part 3, 1978, pp. 545-566.

12 Kim, J., S. J. Kline, and J. P. Johnston, "Investigation of Separation and Reattachement of a Turbulent Shear Layer: Flow over a Backward-Facing Step," MD-37, 1978, Thermosciences Division, Dept. of Mechanical Engineering, Stanford University.

13 Chui, G. K., and S. J. Kline, "Investigation of a Two-Dimensional, Fully Stalled Turbulent Flow Field," MD-19, 1967, Thermosciences Division, Dept. of Mechanical Engineering, Stanford University.

14 Hussain, A. K. M., and W. C. Reynolds, "The Mechanics of a Perturbation Wave in Turbulent Shear Flow," FM-6, 1970, Thermosciences Division, Dept. of Mechanical Engineering, Stanford University.

15 Fielder, H., and M. R. Head, "Intermittency Measurements in Turbulent Boundary Layer, *Journal of Fluid Mechanics,* Vol. 25, Part 4, 1966, pp. 719-735.

16 Eaton, J. K., J. P. Johnston, and A. H. Jeans, "Measurements in a Reattaching Turbulent Shear Layer," presented at the Second Symposium on Turbulent Shear Flows," July 2-4, 1979, Imperial College of Science and Technology, London, England.

17 Kline, S. J., and. A. McClintock, "Describing Uncertainty in Single-Sample Experiments," Mechanical Engineering Department, Stanford University, Jan. 1953.

18 Schraub, F. A., and S. J. Kline, "A Study of the Structure of the Turbulent Boundary Layer with and without Longitudinal Pressure Gradients," MD-12, March 1965, Thermosciences Division, Dept. of Mechanical Engineering, Stanford University.

19 Bradshaw, P., and J. Murlis, "On the Measurement of Intermittency in Turbulent Flow," IC Aero Report 74-04, March 1974, Dept. of Aeronautics, Imperial College of Science and Technology, London, England.